Quantitative measurement of lymphatic function in mice by noninvasive near-infrared imaging of a peripheral vein

Steven T. Proulx, Qiaoli Ma, Diana Andina, Jean-Christophe Leroux, and Michael Detmar

Institute of Pharmaceutical Sciences, Swiss Federal Institute of Technology, ETH Zurich, Zurich, Switzerland.

Optical imaging methods have been developed to measure lymphatic function in skin; however, the lymphatic system of many organs is not accessible to this technology. Since lymphatic transport of macromolecules from any organ proceeds to the blood circulation, we aimed to develop a method that can measure lymphatic function by monitoring the fluorescence in a superficial vein of an interstitially injected tracer. We selected a 40-kDa PEGylated near-infrared dye conjugate, as it showed lymphatic system–specific uptake and extended circulation in blood. Lymphatic transport to blood from subcutaneous tissue required a transit time before signal enhancement was seen in blood followed by a steady rise in signal over time. Increased lymphatic transport was apparent in awake mice compared with those under continuous anesthesia. The methods were validated in K14-VEGFR-3-Fc and K14-VEGF-C transgenic mice with loss and gain of lymphatic function, respectively. Reduced lymphatic transport to blood was also found in aged mice. The technique was also able to measure lymphatic transport from the peritoneal cavity, a location not suitable for optical imaging. The method is a promising, simple approach for assessment of lymphatic function and for monitoring of therapeutic regimens in mouse models of disease and may have potential for clinical translation.

Introduction

The lymphatic vascular system is important for maintaining fluid homeostasis, for the transport of macromolecules from the interstitial tissue to the blood, and for modulation of immunity in tissues. It has been shown to play key roles in many disorders such as cancer, chronic inflammation, and lymphedema (1). The increasing number of pathologies being linked to the lymphatic system has highlighted the need for standardized techniques that can measure lymphatic function in many different organs in mouse models of disease as well as in the clinic.

Several methods have recently been developed to measure lymphatic function in vivo (2). Near-infrared (NIR) imaging has been especially helpful in this regard, as it has enabled quantitative measures in mice of lymphatic clearance from skin, collecting lymphatic vessel contractility, and flow to or through peripheral lymph nodes (3–6). Translation to humans using clinically approved indocyanine green (ICG) is well underway, with many groups using this noninvasive imaging technique to map lymphatic flow routes or to measure collecting lymphatic vessel pumping pressure in superficial regions of the skin (7–9). For overall assessment of lymphatic outflow, optical imaging of a region of interest containing collecting vessels or lymph nodes will only show part of the picture, as the lymphatic drainage routes in many regions of the body are complex. In addition, because of its limited penetration depth, lymphatic flow from deeper organs such as the peritoneal cavity, heart, lung, and brain cannot be measured using optical imaging techniques.

Lymphatic vessels from all regions of the body lead to junctions with the blood vascular system at either the right or left subclavian vein. Previous investigators have attempted to take advantage of this "all roads lead to Rome" property of the lymphatic system by monitoring the levels of radiolabeled or fluorescently labeled macromolecules in the bloodstream after injections into interstitial tissue or a serous cavity (10–13). These assays used cannulation of an artery or vein in order to sample blood at given time points. We have previously shown that long-circulating NIR tracers can be noninvasively visualized in large blood vessels under the skin of mice, enabling the quantification of blood vascular leakage (14). Therefore, we hypothesized that noninvasive monitoring of signals from NIR fluorescent tracers in a superficial blood
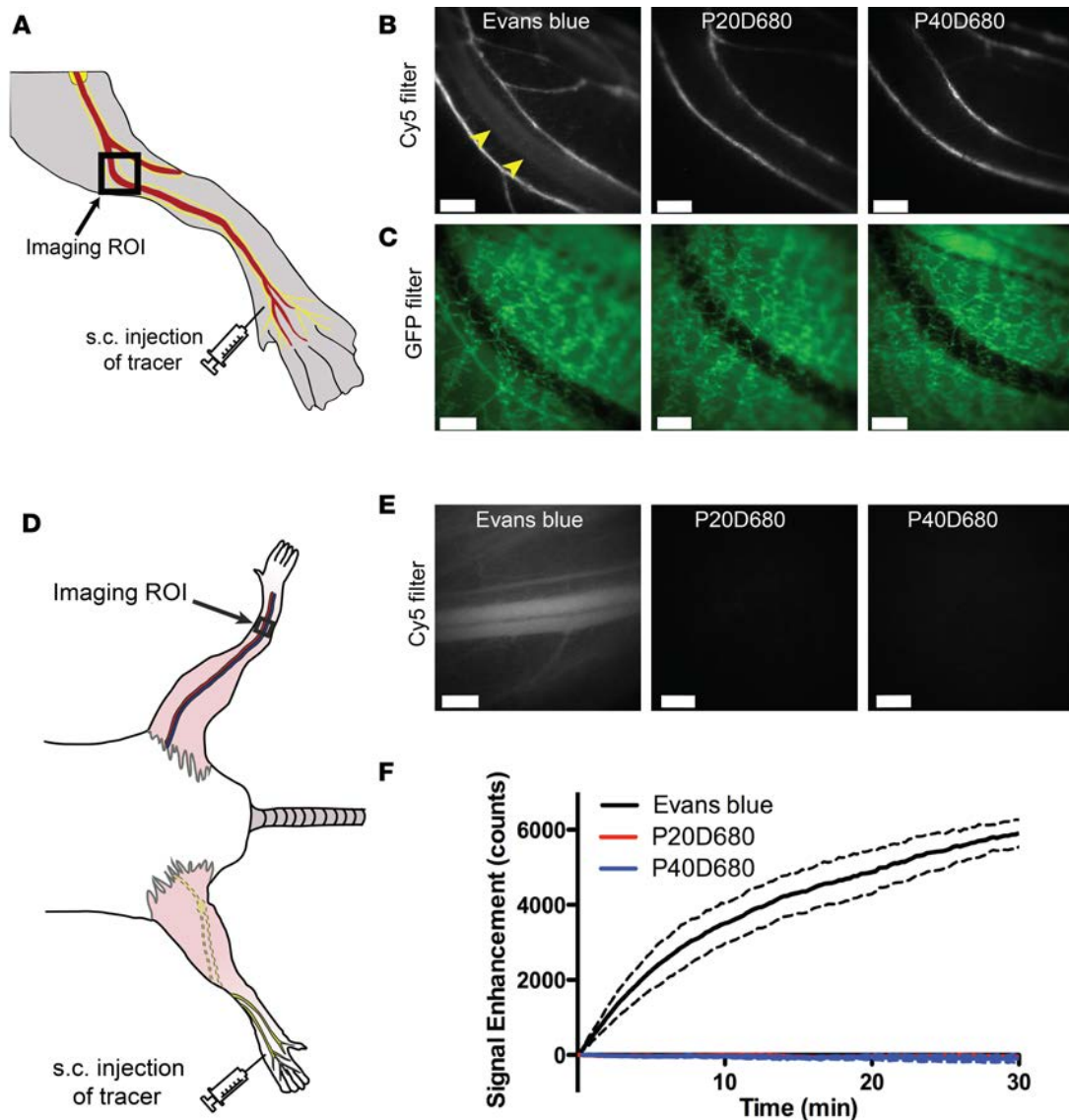
**Figure 1. Lymphatic specificity of potential imaging tracers.** (**A**) Schematic showing s.c. injection site on dorsal aspect of the paw and location of imaging region of interest (ROI) containing popliteal vein with adjoining collecting lymphatic vessels with mouse in prone position. (**B**) Representative video frames after s.c. injections of 2% Evans blue (20 μl), a 20-kDa PEG–IRDye680 conjugate (P20D680), and a 40-kDa PEG–IRDye680 conjugate (P40D680) (20 μl of 25 μM each). Uptake of Evans blue into popliteal vein (yellow arrowheads) as well as collecting lymphatic vessels was seen. P20D680 and P40D680 uptake was solely into collecting lymphatic vessels. Each image is representative of n = 3 mice per tracer. (**C**) Corresponding Prox1-GFP images of regions shown in **B**. Scale bars: 500 μm. (**D**) Schematic showing s.c. injection site on dorsal aspect of the paw and location of imaging ROI of the saphenous vein on the contralateral leg with mouse in supine position. (**E**) Representative video frames showing Evans blue signal in saphenous vein at t = 5 minutes after s.c. injection with no P20D680 or P40D680 signals in saphenous vein at the same time point. Scale bars: 500 μm. (**F**) Signal enhancement curve over time after s.c. injections of Evans blue, P20D680, and P40D680. n = 3 mice for each tracer. Dashed lines show SD.

vessel after interstitial injection might represent a new strategy to dynamically quantify lymphatic function. Thus, an interstitially injected lymphatic system–specific tracer will require a certain transit time to appear in the bloodstream and then will slowly accumulate over time if it avoids retention in the lymph nodes and has a long serum half-life.

In this study, we identified a suitable NIR tracer by providing evidence of its lymphatic specificity and stability in serum. With this probe, we established an imaging technique that allows highly sensitive detection of changes in tracer blood levels. Next, we studied the effects of anesthesia and tissue movement on lymph formation after subcutaneous injections of tracer in the paw. We then applied the assay to 2 transgenic mouse models, K14-VEGFR-3-Fc mice with defects in lymphatic function and K14-VEGF-C mice with increased skin lymphatic vessel density and clearance. The assay was also able to detect a reduction in
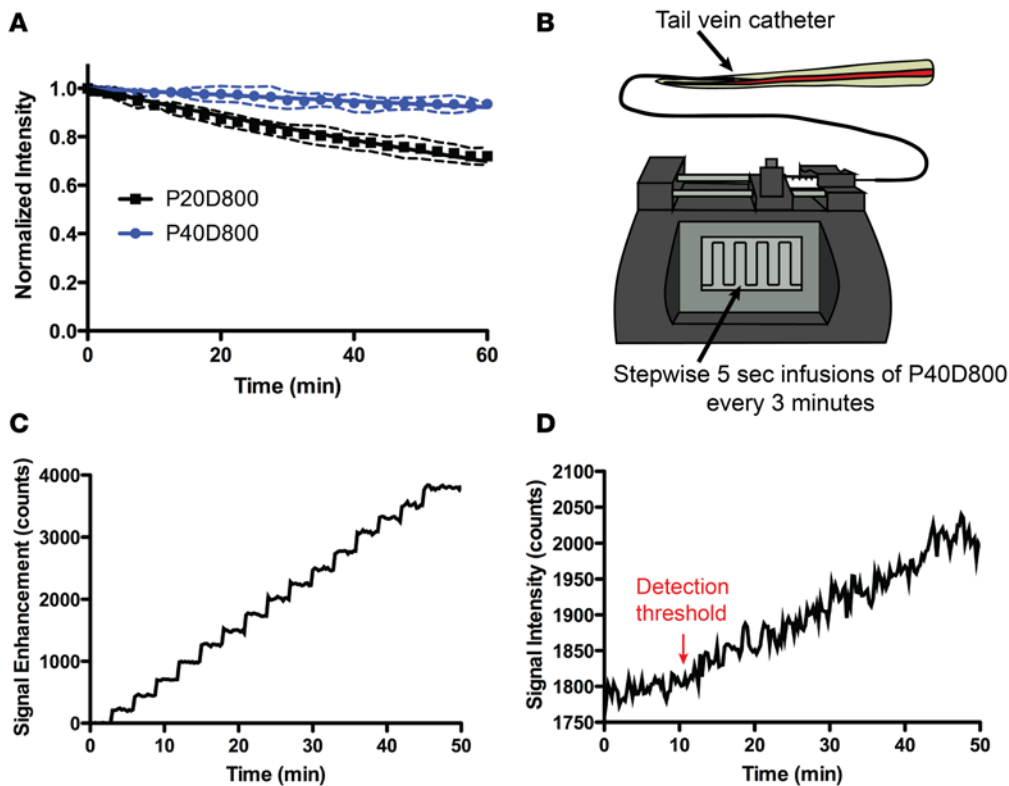
Figure 2. Determination of tracer fluorescent signal kinetics and sensitivity of detection in blood. (**A**) Monitoring of saphenous vein signals after tail vein injections of 20-kDa PEG–IRDye800 conjugate (P20D800) or 40-kDa PEG–IRDye800 conjugate (P40D800) (25 μl of 40 μM each). $n = 4$ mice each tracer. (**B**) Schematic showing stepwise tail vein infusion setup to determine sensitivity of detection in blood of P40D800 tracer. (**C**) Plot showing saphenous vein signal enhancement during stepwise infusions of 10 μl of 1 μM P40D800. Representative of $n = 3$ independent experiments. (**D**) Plot showing saphenous vein signal during stepwise infusions of 10 μl of 0.1 μM P40D800. Representative of $n = 4$ independent experiments. Detection threshold indicates time point where signal increase is first detected after 3 infusions of 0.1 μM P40D800.

lymphatic transport to blood in aged 18-month-old mice compared with young 2-month-old mice. Finally, we applied the technique to the peritoneal cavity and found that lymphatic transport can be quantified from this location. In sum, we have successfully developed a method that allows dynamic measurements of lymphatic function after injection of a NIR lymphatic system–specific tracer into potentially any organ or serous cavity.

Results

Selection of a suitable tracer for lymphatic transport quantifications. Evans blue dye has been used in many previous reports as an indicator of lymphatic function (15) and, in some cases, absorbance measures of Evans blue dye in serum at a time point after interstitial administration have been used as an assessment of lymphatic transport (16, 17). As Evans blue dye is inexpensive, widely available, and has fluorescence in the NIR range using Cy5 filters, we therefore tested this dye as a potential tracer for noninvasive monitoring of lymphatic transport in comparison with custom-made 20-kDa PEG–IRDye680 (P20D680) and 40-kDa PEG–IRDye680 (P40D680) conjugates, which can be imaged with the same filter sets (18). We first tested lymphatic specificity by acquiring videos with a stereomicroscope of the downstream popliteal vein and collecting lymphatic vessels after subcutaneous injection into the dorsal aspect of the paw in Prox1-GFP albino mice (Figure 1A). Using this protocol, we found immediate venous uptake after injection of 20 μl of 2% Evans blue (Figure 1, B and C, and Supplemental Video 1; supplemental material available online with this article; doi:10.1172/jci.insight.90861DS1). In contrast, after injecting 20 μl of 25 μM P20D680 or P40D680 into the paw, we did not detect any uptake into the popliteal vein (Figure 1, B and C, and Supplemental Video 2). For all 3 tracers, efficient uptake into the collecting lymphatic vessels was typical only after massage of the injection site.

Similar results were obtained when monitoring the saphenous vein on the contralateral side from the injected paw as a measure of the tracer in the systemic circulation (Figure 1D). Signal was seen within 30 seconds after the subcutaneous injection of 2% Evans blue into the paw, with the fluorescence increasing throughout the 30-minute course of the experiment (Figure 1E and Supplemental Video 3). These results imply that not all injected Evans blue binds albumin or other proteins in interstitial tissue and that the remaining free dye can be directly absorbed into the venous system. In contrast, both P20D680 and P40D680 did not show any blood signals above tissue background levels after subcutaneous injection, indi-
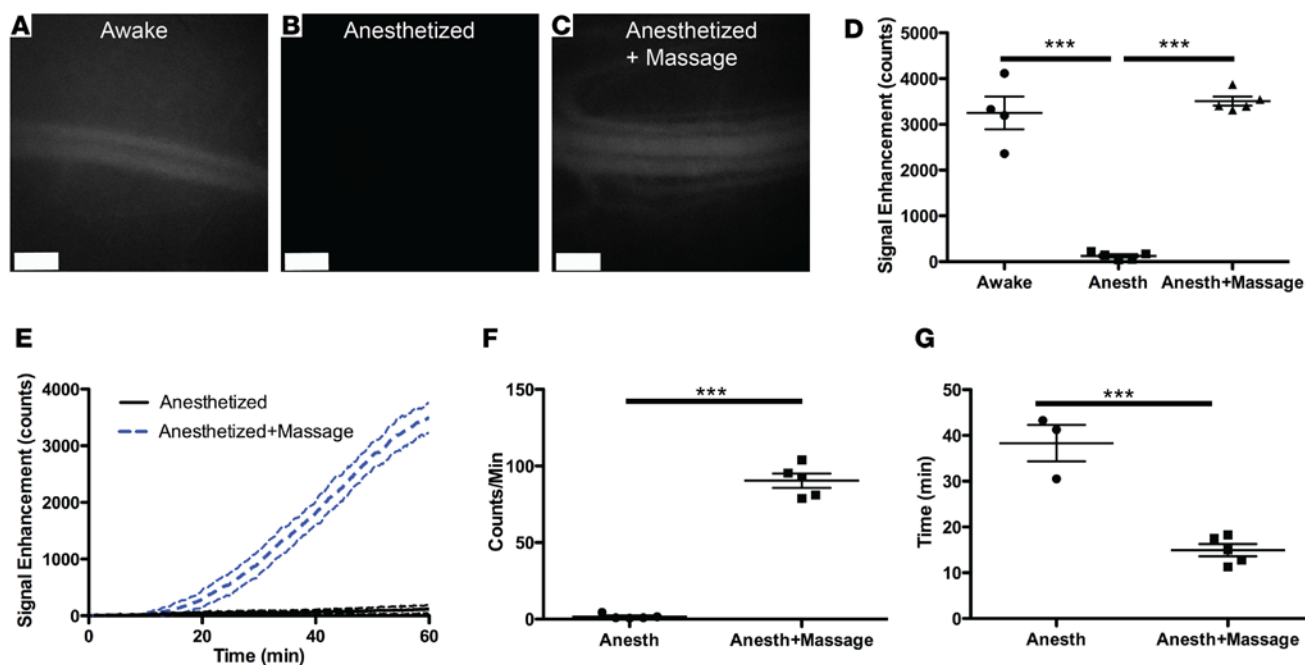
Figure 3. Effects of anesthesia and massage on lymphatic uptake from the paw. Nine-week-old female albino C57BL/6J mice were s.c. injected with 5 μl of 200 μM 40-kDa PEG–IRDye800 conjugate (P40D800) in the dorsal aspect of the right rear paw. (**A**–**C**) Representative saphenous vein images 60 minutes after s.c. injection of P40D800, during which mice were awake and moving normally (**A**), were anesthetized (**B**), or after s.c. injection of P40D800 during anesthetized conditions with the paw massaged for 10 seconds every 5 minutes from t = 5 to 50 minutes (**C**). Scale bars: 500 μm. (**D**) Quantification of the P40D800 fluorescent signal enhancement at t = 60 minutes showed comparable signals between mice that were awake and those that were massaged; however, very little enhancement was observed in unmanipulated anesthetized mice. (**E**) Dynamic imaging showed that the mice that were massaged had steady enhancement of signal starting at around t = 15 minutes after tracer injection until t = 60 minutes. Dashed lines indicate SD. n = 5 each condition. (**F**) Linear slope of signal enhancement from t = 30 to 45 minutes. (**G**) Time of arrival of tracer to the blood circulation (set at a threshold of 100 counts of signal enhancement). Two of 5 mice in the anesthetized group did not reach this threshold. ***$P < 0.001$ using 1-way ANOVA with Tukey's multiple comparison test (**D**) or 2-tailed Student's t test (**F** and **G**). Data are the mean ± SD.

cating that the tracer remained in the interstitial tissue or showed only limited transport by the lymphatic system (Figure 1E). Quantification (Figure 1F) demonstrated an immediate steady increase in saphenous vein signal after Evans blue injection, indicating that this dye is not suitable for quantification of lymphatic transport to blood.

Unexpectedly, a slight loss of the background tissue signal was apparent over time in P20D680- and P40D680-injected mice. This effect was due to photobleaching of endogenous tissue autofluorescence from continuous excitation by the LED light source at 635 nm, as it was also evident in mice that were not injected with tracers (Supplemental Figure 1). This photobleaching effect was not seen with the 770-nm excitation wavelength and the ICG filter set used for IRDye800 (D800) conjugates, owing to lower tissue autofluorescence at these wavelengths. Since accurate quantification of lymphatic transport to blood in a dynamic manner would require stable background signals at the saphenous vein, D800 conjugates are better suited for dynamic imaging and were selected for the subsequent studies.

The 40-kDa PEG tracers demonstrate stable fluorescence in blood and excellent sensitivity for NIR detection and quantification. For monitoring of signal in the blood, it is attractive to have tracers with a longer half-life so that lymphatic transport is not underestimated due to elimination through the kidneys or by blood vascular leakage into interstitial tissue. Previously we measured serum half-lives of 2.4 ± 0.7 hours for P20D800 and 12.6 ± 4.3 hours for P40D800 (14). Since we intend to monitor the fluorescence in the vein over the course of an hour during measurements of lymphatic function, we estimated the loss of signal in the saphenous vein over a 60-minute period. We injected 25 μl of either P20D800 or P40D800 (both 40 μM) in the tail vein and measured 28.0% ± 3.6% loss of P20D800 and 6.4% ± 2.1% loss of P40D800 at 60 minutes (Figure 2A). This indicates that 40-kDa conjugates will exhibit negligible clearance of signal from the blood while measurements of lymphatic transport to blood are performed.

To confirm that the NIR imaging signal is an accurate reflection of the amount of tracer in the blood-
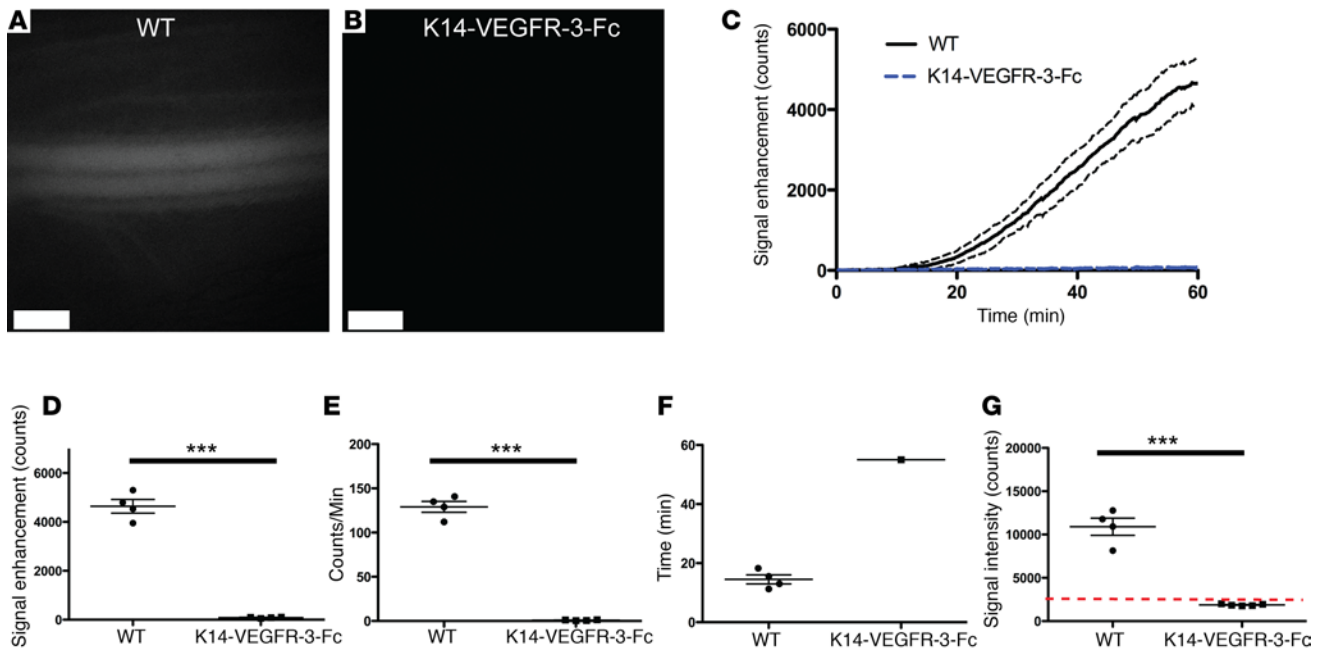
Figure 4. Limited lymphatic transport in K14-VEGFR-3-Fc mice compared with WT littermates. Twelve-week-old female K14-VEGFR-3-Fc or WT littermates were s.c. injected with 5 μl of 200 μM 40-kDa PEG–IRDye800 conjugate (P40D800) in the dorsal aspect of the right rear paw. (**A**) Representative saphenous vein signal in a WT mouse 60 minutes after s.c. injection of P40D800 during anesthetized conditions with the paw massaged for 10 seconds every 5 minutes from t = 5 to 50 minutes. (**B**) Representative saphenous vein signal in a K14-VEGFR-3-Fc mouse under the same conditions. Scale bars: 500 μm. (**C**) Saphenous vein signal enhancement plots of K14-VEGFR-3-Fc and WT mice (n = 4 each). Dashed lines indicate SD. (**D**) Quantification of the fluorescent signal enhancement at t = 60 minutes. (**E**) Linear slope of signal enhancement from t = 30 to 45 minutes. (**F**) Time of arrival of tracer to the blood circulation (set at a threshold of 100 counts of signal enhancement). Three of 4 mice in the K14-VEGFR-3-Fc group did not reach this threshold. (**G**) Quantification of fluorescent signal from a 40-kDa PEG–IRDye680 conjugate (P40D680) at t = 60 minutes after s.c. injection, during which mice were awake and moving normally. K14-VEGFR-3-Fc mice showed signal at baseline levels (red dashed line) indicating no transport to blood. ***P < 0.001 (2-tailed Student's t test). Data are the mean ± SD.

stream, it is necessary to show that the recorded signal increases as expected when known quantities of dye are introduced into the system. We therefore tested this by measuring the signal response to repeated intravenous infusions of 0.01 nmol P40D800 once every 3 minutes using an implanted tail vein catheter (Figure 2B). A consistent step-wise increase in signal was found with each infusion that averaged 255.2 ± 22.7 counts (Figure 2C and Supplemental Video 4). This average increase in signal was also very consistent between mice (mean ± SD = 261.3 ± 5.6 counts; n = 3). We then determined the minimum concentration of tracer that could be detected in the blood using the noninvasive imaging setup by repeating the timed infusions with a lower dose of 0.001 nmol P40D800 in n = 4 mice. A signal increase was consistently detected after 0.003 nmol P40D800 had been infused (Figure 2D). Based on this result we decided to set the dose of P40D800 for interstitial administration to 1 nmol, meaning that the detection threshold in blood would represent approximately 0.3% of the injected dose in a 20-g mouse.

Quantification demonstrates the effects of anesthesia and massage on lymph formation in the extremities. We next tested if we could detect lymphatic transport to blood of P40D800 after subcutaneous injection in the rear paw with the mouse under awake or anesthetized conditions. Nine-week-old albino C57BL/6J-Tyr[c-J] mice were subcutaneously injected with 5 μl of 200 μM P40D800 in the dorsal aspect of the right rear paw, and the signal in the left saphenous vein at t = 60 minutes after injection was compared between mice that were awake (Figure 3A) or were anesthetized with ketamine/medetomidine (Figure 3B). Signal was readily apparent in the mice that had been awake, but no signal above background levels could be seen in the mice under anesthetized conditions. Lymph formation in the extremities is highly dependent on extrinsic factors such as muscular activity (19). These forces driving flow into initial lymphatic vessels are considered to be inactive when the mouse is at rest, such as during anesthesia (20). To test if tissue massage could stimulate lymphatic uptake, we massaged the injection site at the paw for 10 seconds every 5 minutes from t = 5 to 50 minutes while the mouse was anesthetized with ketamine/medetomidine. Under these conditions,
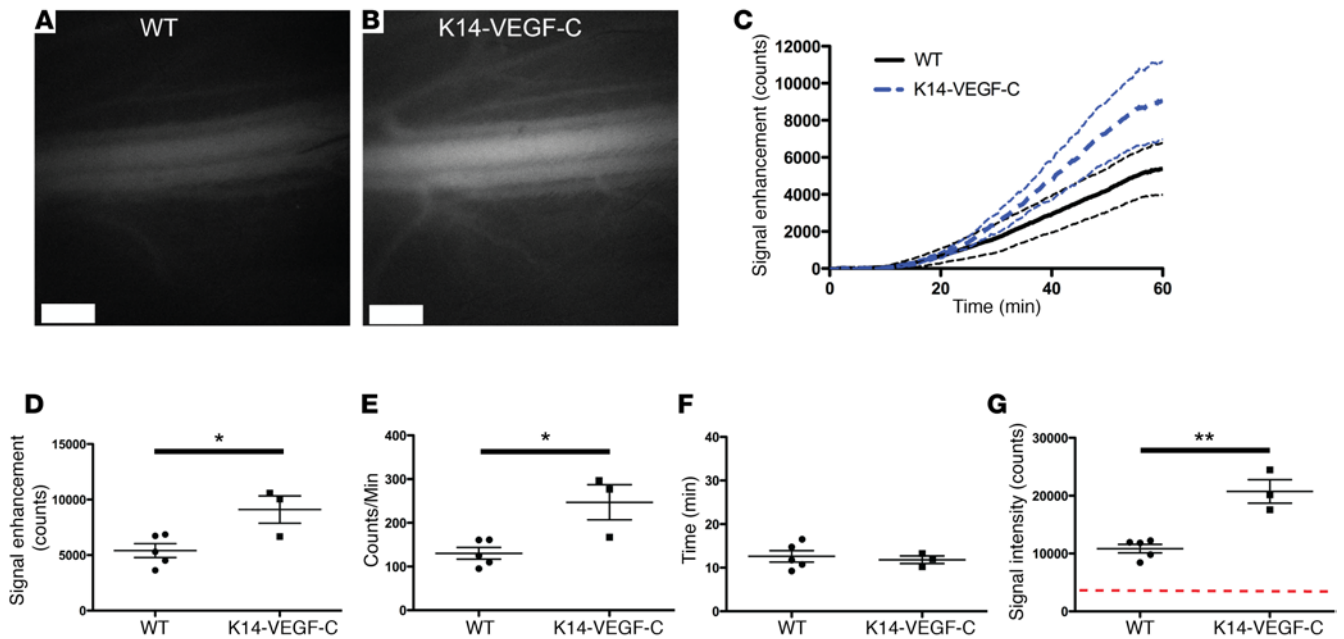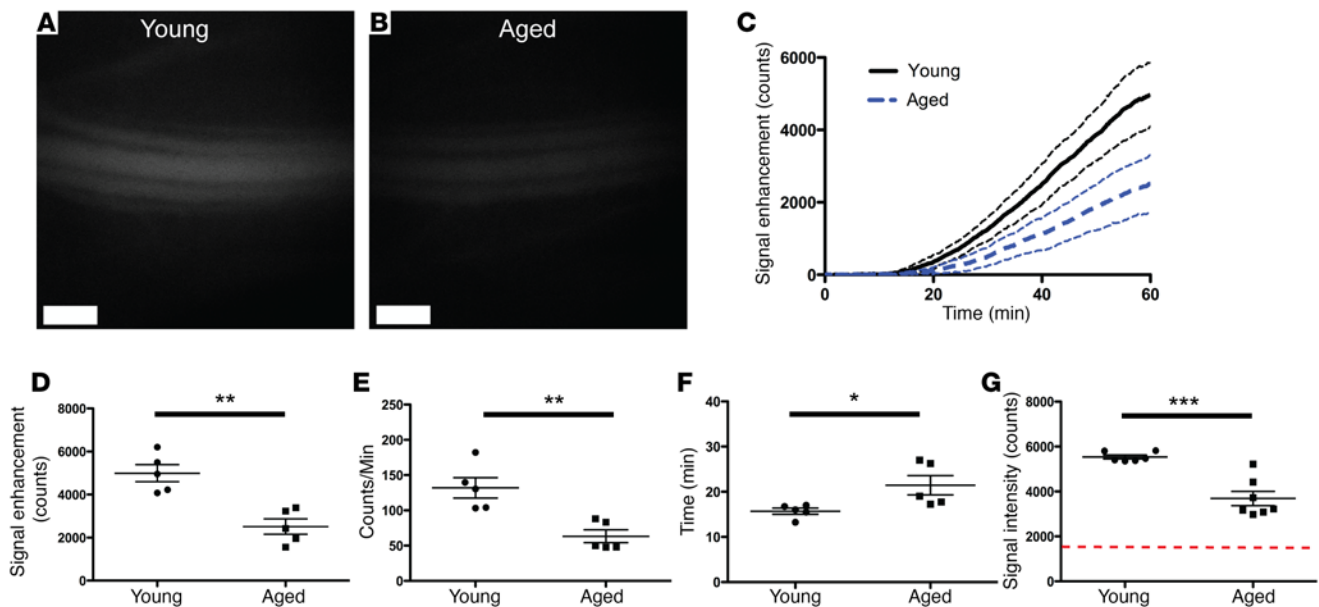
Figure 5. Increased lymphatic transport in K14-VEGF-C mice compared with WT littermates. Twelve-week-old female K14-VEGF-C or WT littermates were s.c. injected with 5 μl of 200 μM 40-kDa PEG–IRDye800 conjugate (P40D800) in the dorsal aspect of the right rear paw. (**A**) Representative saphenous vein image in a WT mouse 60 minutes after s.c. injection of P40D800 during anesthetized conditions with the paw massaged for 10 seconds every 5 minutes from t = 5 to 50 minutes. (**B**) Representative saphenous vein image in a K14-VEGF-C mouse under the same conditions. Scale bars: 500 μm. (**C**) Saphenous vein signal enhancement plots of K14-VEGF-C (n = 3) and WT (n = 5) mice. Dashed lines indicate SD. (**D**) Quantification of the fluorescent signal enhancement at t = 60 minutes. (**E**) Linear slope of signal enhancement from t = 30 to 45 minutes. (**F**) Time of arrival of tracer to the blood circulation (set at a threshold of 100 counts of signal enhancement). (**G**) Quantification of fluorescent signal from a 40-kDa PEG–IRDye680 conjugate (P40D680) at t = 60 minutes after s.c. injection, during which mice were awake and moving normally. Red dashed line indicates baseline signal level. *P < 0.05, **P < 0.01 (2-tailed Student's t test). Data are the mean ± SD.

we could easily detect signal in the saphenous vein at 60 minutes (Figure 3C). We recorded videos of the downstream collecting lymphatic vessels during this massage protocol that showed a consistent response of increased signal in the vessels with each massage and demonstrated the active contractility of these vessels (Supplemental Video 5). Quantification of the NIR fluorescent signal enhancement at the saphenous vein at t = 60 minutes (Figure 3D) showed comparable signals between mice that were awake and those that were massaged under anesthesia; however, very little enhancement was observed in the unmanipulated, anesthetized mice.

The dynamics of lymphatic transport should demonstrate a delay in the appearance of the signal in blood during the time that the tracer is transported by the lymphatic system from interstitial tissue to the junction(s) at the subclavian veins, followed by a steady increase in signal as more and more tracer is transported. Dynamic imaging (Figure 3E and Supplemental Video 6) was possible for the 2 groups under anesthesia and the mice that were massaged showed an initial enhancement of signal starting at around t = 15 minutes after tracer injection, followed by a steady increase in signal until t = 60 minutes. Quantification was developed to track the linear slope of signal enhancement from t = 30 to 45 minutes (Figure 3F) and to track the transit time until arrival of tracer in the blood circulation (set at a threshold of 100 counts of signal enhancement) (Figure 3G). Both measures showed that more tracer was transported during the massage protocol, indicating that the assay is able to quantitatively assess the effects of tissue movement during anesthesia on initial lymphatic uptake.

K14-VEGFR-3-Fc mice lacking dermal lymphatic vessels show essentially no lymphatic transport. We next tested our methods in a mouse model with reduced lymphatic clearance from skin, K14-VEGFR-3-Fc mice (5, 21). These mice lack lymphatic vessels in the dermis; however, lymphatic structures and drainage function are retained in deeper tissues (22). Blood vessel signal was monitored in K14-VEGFR-3-Fc and wild-type littermates after subcutaneous injection of 1 nmol P40D800 into the right paw and utilization of the massage protocol described above. At 60 minutes there was obvious signal in the saphenous vein of wild-type

Figure 6. Decreased lymphatic transport in aged mice compared with young controls. Eighteen-month-old (aged) or 2-month-old (young) female C57BL/6J-Tyr^{c-J} albino mice were s.c. injected with 5 μl of 200 μM 40-kDa PEG–IRDye800 conjugate (P40D800) in the dorsal aspect of the right rear paw. (**A**) Representative saphenous vein image of a young mouse 60 minutes after s.c. injection of P40D800 during anesthetized conditions with the paw massaged for 10 seconds every 5 minutes from t = 5 to 50 minutes. (**B**) Representative saphenous vein image of an aged mouse under the same conditions. Scale bars: 500 μm. (**C**) Saphenous vein signal enhancement plots of young and aged mice (n = 5 each). Dashed lines indicate SD. (**D**) Quantification of the fluorescent signal enhancement at t = 60 minutes. (**E**) Linear slope of signal enhancement from t = 30 to 45 minutes. (**F**) Time of arrival of tracer to the blood circulation (set at a threshold of 100 counts of signal enhancement). (**G**) Quantification of P40D800 fluorescent signal at t = 60 minutes after s.c. injection. Mice were awake and moving normally between the time of injection and imaging (n = 6 young, n = 7 aged). Red dashed line indicates baseline signal level. *$P < 0.05$, **$P < 0.01$, ***$P < 0.001$ (2-tailed Student's t test). Data are the mean ± SD.

mice (Figure 4A), with no signal apparent in K14-VEGFR-3 mice (Figure 4B). Quantification of the blood vessel signal (Figure 4C) revealed vastly reduced lymphatic transport of P40D800 in K14-VEGFR-3-Fc mice compared with wild-type littermates, with lower signal enhancement at 60 minutes (79.0 ± 23.0 vs. 4,643.1 ± 560.2 counts, respectively; $P < 0.0001$; Figure 4D) and a decreased slope of enhancement from 30 to 45 minutes (0.9 ± 0.5 vs. 129.1 ± 12.4 counts/min, respectively; $P < 0.0001$; Figure 4E). Three of 4 K14-VEGFR-3-Fc mice did not reach a signal enhancement of 100 counts during the study period, indicating a dramatically increased transit time (Figure 4F). We also tested whether similar differences in lymphatic transport would be found during awake conditions in the same cohort of mice. For this experiment, we used the P40D680 tracer to avoid any interference from the previously injected P40D800. Single images were acquired of the blood vessel signal using the Cy5 filter after K14-VEGFR-3-Fc and wild-type mice had been awake for 60 minutes after injection of 0.5 nmol P40D680 tracer. Wild-type mice displayed significantly higher signal in the saphenous vein than K14-VEGFR-3-Fc mice, which showed signal at baseline levels (10,903 ± 1,991 vs. 1,852 ± 105 counts, respectively; $P < 0.0001$; Figure 4G).

K14-VEGF-C mice with expanded dermal lymphatic vessels show increased lymphatic transport. We next tested the assay in a model with an expected increase in lymphatic function, the K14-VEGF-C model (23). These mice have an increased density of lymphatic vessels in the dermis of the skin and an increased lymphatic clearance (5). Using the massage protocol under anesthesia, we found greater P40D800 signal in the saphenous vein of K14-VEGF-C mice at 60 minutes after subcutaneous injection compared with wild-type littermates (Figure 5, A and B). Quantification over time (Figure 5C) revealed significantly higher signal enhancement at 60 minutes in the K14-VEGF-C group compared with wild type (9,101.4 ± 2,124.7 vs. 5,404.4 ± 1,398.1 counts, respectively; $P = 0.02$; Figure 5D), with an increased slope from 30 to 45 minutes (247.0 ± 69.8 vs. 130.3 ± 30.0 counts/min, respectively; $P = 0.01$; Figure 5E). There was no significant difference in the transit time to the blood between K14-VEGF-C and wild type (11.8 ± 1.5 minutes vs. 12.6 ± 3.0 minutes, respectively; $P = 0.70$; Figure 5F). Experiments in mice that were awake for 60 minutes after subcutaneous injection of 0.5 nmol P40D680 tracer also demonstrated a significant increase in saphenous

vein signal in K14-VEGF-C mice compared with wild-type littermates (20,732 ± 3,496 counts vs. 10,847 ± 1,655 counts, respectively; $P = 0.001$; Figure 5G).

Aged mice show reduced lymphatic transport compared with young mice. We have previously reported that aged mice have decreased lymphatic clearance from ear skin compared with young controls, corresponding with a loss of lymphatic vessel density in the aged skin (5). Therefore, we evaluated whether the new assay could detect differences in lymphatic transport in 18-month-old (aged) and 2-month-old (young) C57BL/6J-Tyr[c-J] albino mice. We detected less P40D800 signal in the saphenous vein of aged mice at 60 minutes after subcutaneous injection, using the massage protocol under anesthesia, compared with young controls (Figure 6, A and B). Quantification from dynamic imaging (Figure 6C) revealed a significant reduction in signal enhancement at 60 minutes in aged mice compared with young mice (2,512.0 ± 793.5 vs. 4,993.0 ± 886.5 counts, respectively; $P = 0.002$; Figure 6D). Aged mice also showed a significantly decreased slope of enhancement from 30 to 45 minutes (63.3 ± 20.4 vs. 131.9 ± 32.4 counts/min, $P = 0.004$, Figure 6E) and a significant increase in transit time to blood (21.5 ± 4.8 vs. 15.7 ± 1.5 min, $P = 0.03$, Figure 6F) compared with young mice. An experiment performed in additional cohorts of aged and young mice under awake conditions showed similar results, with a reduction in lymphatic transport to blood of P40D800 at 60 minutes (aged: 3,687.0 ± 837.9 counts; young: 5,537.0 ± 213.9 counts; $P < 0.001$; Figure 6G).

Lymphatic transport can be monitored after i.p. injection. Finally, we tested the potential of the assay in an anatomical location of the mouse where it is difficult to visualize the lymphatic outflow using in vivo optical methods. We chose the peritoneal cavity, as many different outflow routes have been described including uptake through stomata in the diaphragm and by omental lymphatics of the abdomen (19, 24–26). After i.p. injection of 1 nmol P40D800, we were able to track the enhancement in blood signal after a delay of around 20 minutes (Figure 7, A and B), indicating that the 40-kDa tracer is not taken up directly by blood vessels lining the peritoneal space. Validation of lymphatic outflow pathways using P40D680 tracer in Prox1-GFP mice showed tracer present in the diaphragmatic and paravertebral lymph vessels and in the tracheobronchal and right mediastinal lymph nodes (Figure 7, C–E). Signal was also detected in the thoracic duct. We then tested if similar effects of anesthesia would be found at this location, as we speculated that since the diaphragmatic movement of the breathing is retained, there may not be as large effects as those seen in the periphery. However, we found that there was a dramatic decrease in lymphatic transport seen in anesthetized mice as opposed to awake mice (447.4 ± 304.6 vs. 7,814.3 ± 901.7 counts, respectively; $P < 0.0001$; Figure 7, F–H). In conclusion, the assay can track lymphatic transport from the peritoneal cavity; however, in the future it may be necessary to perform assessments of lymphatic transport to blood with mice that are awake for a time period after the injection of tracer.
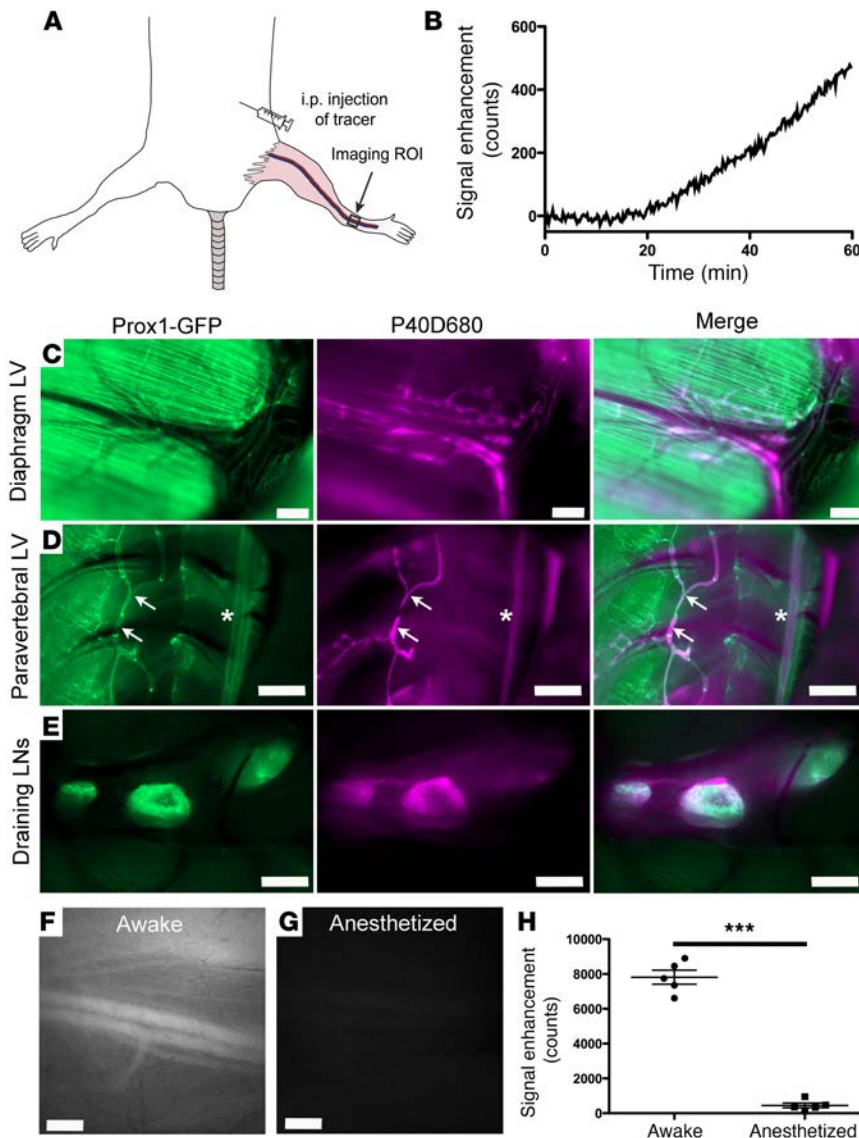
Discussion

In this study, we have developed a potentially new technique to quantitatively assess lymphatic function in mice. We have identified a suitable tracer, P40D800, with stable fluorescent signals after intravenous injection and specificity for lymphatic uptake from interstitial tissue. By monitoring the blood signal of this tracer after interstitial injections using NIR imaging, a simple method to dynamically measure lymphatic function was established. We showed the influence of anesthesia and animal movement on lymph formation in the peripheral extremities. The assay was successfully applied to the peritoneal cavity, indicating that functional assessments of lymphatic transport from deeper tissues may now be performed in mice.

Many early studies to measure lymphatic flow involved surgical approaches to cannulate collecting lymphatic vessels for measurement of flow rates of interstitially injected tracers. These methods were mostly performed in large animals, such as dog, cow, sheep, and, in some cases, have even been carried out in humans (20, 27–29). However, for many organs the lymphatic outflow pathways are complicated and, therefore, many vessels would require cannulation to accurately measure lymphatic transport. Another potential issue with these techniques is that there may be effects of cannula insertion on flow rates. In addition, in mice lymphatic vessels are too small to be routinely cannulated, so other approaches are necessary in this species.

An alternative approach to lymphatic cannulation was developed in the late 1940s by Courtice and colleagues. Their approach in both cat and rabbit models was to incubate Evans blue dye (then known as T-1824) with the animals own plasma and then to inject the labeled serum proteins into either the pleural or peritoneal cavity (10, 30). From the femoral artery in cats and an ear vein in rabbits, they extracted blood at different time points and absorbance of the dye was used to estimate the lymphatic transport of the protein as a percentage of injected dose (after an adjustment was made to the animal's estimated blood

Figure 7. Lymphatic transport can be tracked from the peritoneal cavity. (**A**) Nine-week-old albino female C57BL/6J mice were i.p. injected with 50 μl of 20 μM 40-kDa PEG–IRDye800 conjugate (P40D800) and dynamic imaging of the saphenous vein signal region of interest (ROI) was performed with the mouse in the supine position. (**B**) Plot showing saphenous vein signal enhancement during anesthetized conditions. Representative of $n = 5$ mice. (**C**–**E**) Images of peritoneal lymphatic outflow 30 minutes after injection of 50 μl of 10 μM 40-kDa PEG–IRDye680 conjugate (P40D680). Left images, Prox1-GFP; middle images, P40D680; right images, merge. Representative of $n = 4$ mice. (**C**) Presence of P40D680 in diaphragmatic lymphatic vessels (LVs). Prox1 is expressed also in diaphragmatic muscle. Scale bars: 500 μm. (**D**) P40D680 in para-vertebral LVs (arrows) and thoracic duct (stars). Scale bars: 1 mm. (**E**) P40D680 in tracheobronchal (right lymph node [LN]) and 2 mediastinal LNs. Scale bars: 1 mm. (**F**) Representative saphenous vein image at $t = 60$ minutes after i.p. injection, during which mice were awake and moving normally. (**G**) Representative saphenous vein image at $t = 60$ minutes after i.p. injection with mouse under anesthesia. Scale bars: 500 μm. (**H**) Quantification of the fluorescent signal enhancement at $t = 60$ minutes comparing mice that were awake with those that were under anesthesia. $n = 5$ each condition. ***$P < 0.001$ (2-tailed Student's t test). Data are the mean ± SD.

volume). This experimental approach was also attempted in dogs (31). However, during these studies it could not be excluded that the protein-dye complexes directly entered blood capillaries or that a significant amount of the protein-dye complexes disappeared from the circulation over time. In addition, it is unknown how stable these complexes are in the interstitial tissue/serous cavity and the blood; i.e., there may be disassociation of dye occurring over time or some Evans blue may not be binding serum proteins at all (32).

Importantly, the approach described here, using 40-kDa PEG-dye conjugates, addresses such concerns. First, very little signal in blood was seen in anesthetized mice after subcutaneous injection into the paw without massage. If tracer could enter blood capillaries, signal would be seen immediately in the bloodstream after injection, as evident with subcutaneous injections of free Evans blue dye. Further confirmation of the specificity of the 40-kDa tracer for dermal lymphatic vessels is provided by the absence of any obvious transport to blood within 1 hour in K14-VEGFR-3-Fc mice that lack lymphatics in the skin, even after multiple manipulations of the paw. However, it should be noted that the specificity of a particular tracer for lymphatic uptake could conceivably be altered in pathological situations, such as inflammation, or in different organs, such as the liver. Secondly, we confirmed the stability of tracer in blood by monitoring the saphenous vein signals over a 60-minute period after intravenous injection. We found a minimal loss of signal of the 40-kDa tracer over the course of 60 minutes, which confirms the previously observed extended serum half-life of P40D800 (14). This indicates that very little signal is lost from the blood during measurements of lymphatic transport due to renal clearance of tracer. Third, we have previously shown that the PEG-dye conjugates are stable in vivo and are excreted in intact form by the kidneys (14).

The major advantage of our technique compared with earlier approaches is that measurements can be made noninvasively and do not require sampling of lymph or blood to estimate lymphatic flow. Small

volumes (<30 µl) of blood could be repeatedly sampled from either the tail vein or saphenous vein in restrained unanesthetized mice (14); however, it is stressful for the animal and this may affect lymph flow (33, 34). Short-term inhalation anesthesia could be used to limit this effect; however, at least in mice, the dynamics of lymph transport are relatively quick, which would require multiple anesthesia applications and blood samplings within a short period of time. A NIR imaging approach avoids these issues by visualization of the fluorescence intensity of the tracer in a blood vessel through the skin. The studies involving controlled intravenous infusions of set amounts of tracer demonstrated the high sensitivity of the imaging method, since there was a direct relationship between fluorescent signal and tracer concentration in the blood with very consistent step-wise increases in signal after each bolus infusion, and since only minimal amounts of tracer were needed to visualize the signal in the saphenous vein with NIR imaging.

There were dramatic differences in lymphatic transport to blood after subcutaneous injections in the paw between mice that were anesthetized and those that were awake. This is in agreement with previous studies that reported very little lymph formation in animals without movement (20, 28, 35). Under steady-state conditions, extrinsic factors such as muscular movement, breathing, and arterial vasomotion are responsible for the driving forces to propel interstitial fluid and macromolecules into the lymphatic capillaries. We found that we could consistently induce flow of the tracer into the lymphatic vessels in anesthetized mice with massage, similar to previous reports in dogs, sheep, and rabbits (28, 35, 36). This loading of the lymphatic system increased the fluorescent signal within the downstream collecting vessels, leading to a probable increase in intraluminal pressure. A clear response of increased pumping of the collecting vessels immediately after each massage has been observed previously (18). This effect demonstrates that the intrinsic contractility of the collecting lymphatic vessels is conserved under anesthesia with ketamine/medetomidine. Indeed, a consistent increase in signal was seen in the blood vessel after repeated massage, indicating further transport by collecting lymphatic trunks of the tracer through the lymphatic system. However, this may not be the case with all types of anesthesia, as, for example, isoflurane has been shown to depress lymphatic contractility (37).

Lymphatic outflow from the peritoneal cavity has been described as mostly passing through the diaphragmatic stomata and corresponding lymphatic vessels and, therefore, may be dependent on muscular movement of this organ associated with breathing (19, 38). Our results indicated that, unlike after subcutaneous injection, some outflow from the peritoneal cavity continued under anesthetized conditions. However, similar to the periphery, there was a large increase in the lymphatic transport of tracer to blood when the mice were awake compared with when they were anesthetized. It has previously been reported that respiratory movement is reduced in anesthetized animals lying on their back (38, 39). Other investigators have also previously found decreased lymphatic outflow from the peritoneum under anesthesia (40–42) and have speculated that abdominal muscle tone plays a large role in driving flow out of the peritoneum. This concept is in agreement with our findings, although more research is necessary to elucidate the major driving forces for lymphatic flow from this serous cavity.

There are some limitations with the described assay. There are difficulties in standardizing lymphatic flow under anesthesia and the massage protocol utilized may introduce a bias in unblinded studies. Therefore, we recommend performing studies with 2 different-wavelength tracers, 1 with mouse groups that are awake and moving normally and 1 with anesthetized mice. In larger animals or humans, a wearable NIR sensor could be used to monitor the signal in the underlying blood vessels of the skin under controlled conditions in conscious subjects. Such devices have been used in humans to measure ICG levels after intravenous infusion (43). While ICG is the only clinically approved NIR dye, it is not an optimal lymphatic tracer for this assay owing to its lack of lymphatic specificity and short serum half-life (18). The high sensitivity of the P40D800 tracer, as well as the safety profiles of PEGs and IRDye800, may allow for its future use in humans.

In conclusion, NIR imaging methods were established that can sensitively assess lymphatic function by measuring levels in the bloodstream of interstitially injected tracers. While the current study has predominantly validated the assay in physiological situations or mouse models with known modifications in initial lymphatic vessel uptake, the technique will likely also prove useful to measure changes in downstream lymphatic transport, such as alterations in the contractility of collecting lymphatic vessels or disruptions in lymphatic flow that occur in situations such as secondary lymphedema. These techniques will enable preclinical studies with evaluation of lymphatic function in deeper organs, and clinical translation may be feasible.

Methods

Mice. C57BL/6J-Tyr^c-J albino mice (Jackson Laboratories) and Prox1-GFP mice (44) on the C57BL/6J-Tyr^c-J albino background were kept under specific pathogen–free conditions and given chow and water ad libitum until imaging. K14-VEGF-C (23) and K14-sVEGFR-3-Fc mice (22) on an FVB background were provided by Kari Alitalo (University of Helsinki, Finland). For aging studies, C57BL/6J-Tyr^c-J albino mice were aged in house and compared with young animals from the same colony. After the completion of imaging experiments, the mice were euthanized with an overdose of anesthesia (1,000 mg/kg ketamine; 3.5 mg/kg medetomidine) followed by cervical dislocation.

Tracer specificity for lymphatic uptake. Prox1-GFP mice were anesthetized (80 mg/kg ketamine; 0.2 mg/kg medetomidine) and legs were shaved with a razor and depilation cream. A Zeiss StereoLumar.V12 stereomicroscope with AxioVision software and a Photometrics Evolve 512 camera was utilized for imaging. A region of interest at ×25 zoom containing the popliteal vein and collecting lymphatic vessels of the rear limb was localized using the GFP filter. A video was then acquired using a Cy5 filter at an exposure time of 200 ms and a gain setting on the camera of 200. Uptake into either blood or lymphatic vessels was tested after subcutaneous injection of 20 μl of 3 tracers: 2% Evans blue (Sigma-Aldrich), P20D680 at 25 μM, and P40D680 at 25 μM (18).

NIR monitoring of blood vessel signal dynamics. Mice were anesthetized and shaved as described above. The mice were positioned under the StereoLumar.V12 microscope in a supine position on a heating pad to retain body temperature. A region of interest over the saphenous vein was chosen for imaging of the fluorescent signal in the blood. The autofluorescence signal on the GFP channel was used to position the saphenous vein at ×25 zoom. A sequence of images (1 image every 15 seconds for 30 to 60 minutes) was acquired with a Cy5 or ICG filter set to monitor the NIR signal of the saphenous vein. Exposure time and camera gain settings were 500 ms and 300, respectively, for ICG wavelengths and 200 ms and 200, respectively, for Cy5 wavelengths.

Stability and sensitivity measurements of tracers in blood. A custom-designed catheter made with polyethylene-10 (PE-10) tubing (SCI) and a 30-gauge needle was inserted into the tail vein of the mice. The catheter was connected to an infusion pump (PHD2000, Harvard Apparatus) for reproducible bolus infusions of tracer. For stability of the tracer in blood measurements, a 25-μl bolus of 40 μM P20D800 or P40D800 was injected (14) and the blood signal monitored as above. For sensitivity assessments, P40D800 tracer was diluted to 1 μM and a stepwise infusion program was programmed into the infusion pump to infuse 10 μl of tracer every 3 minutes. To determine the threshold of detection, a further dilution of P40D800 dye to 0.1 μM was made and stepwise infusions for blood signal monitoring were performed as above. The number of infusions required before a signal increase was detected in the saphenous vein was recorded.

Assessment of lymphatic transport to blood. For assessment of lymphatic transport from the paws, injections of lymphatic tracer (5 μl of 200 μM P40D800 or 5 μl of 100 μM P40D680) were made into the subcutaneous tissue on the dorsal aspect of the right rear paw (18). Depending on the goals of the experiment, injections were made while the mouse was under either short-term or long-term anesthesia, with isoflurane (2%) or ketamine/medetomidine, respectively. For monitoring of lymphatic transport during awake conditions, mice were allowed to quickly recover from isoflurane anesthesia and move about their cages normally for 60 minutes. After this time, the mice were anesthetized with ketamine/medetomidine to assess the signal in the saphenous vein by stereomicroscopy as described above. For monitoring of lymphatic transport during anesthetized conditions, the mice were monitored under the stereomicroscope in a dynamic manner as described above. To stimulate initial lymphatic vessel uptake during anesthetized conditions, a protocol was developed to massage the injection site with a cotton applicator. Slight pressure was applied to the skin containing the injection bolus once per second for 10 seconds. This was repeated 10 times, from $t = 5$ minutes to $t = 50$ minutes after the subcutaneous injection of the tracer.

For assessment of lymphatic transport from the peritoneal cavity, injections of lymphatic tracer (50 μl of 20 μM P40D800 or 50 μl of 10 μM P40D680) were made i.p. The saphenous vein of mice was imaged as above after awake conditions for 60 minutes or while under anesthesia with ketamine/medetomidine. Anatomical mapping of the outflow pathways in Prox1-GFP mice after sacrifice was performed 30 minutes after i.p. injection of P40D680 using a Zeiss AxioZoom V16 microscope and a QImaging OptiMOS sCMOS camera (QImaging) combined with a pE-4000 LED Illumination System (CoolLED Ltd).

Analysis of NIR signal dynamics. Using AxioVision software, a circular region of interest of radius 100 μm was placed over the saphenous vein on videos acquired using the settings described above (under NIR

monitoring of blood vessel signal dynamics). Using the Measure Profile function, a table of fluorescence intensity in counts versus time was exported into Microsoft Excel. Baseline intensity (an average of 10 recordings prior to injection of tracer) was subtracted in order to plot fluorescent signal enhancement versus time in minutes. For quantification of loss of fluorescent signal at 1 hour after blood vessel injection of different tracers, the peak signal enhancement shortly after injection was set to 100% and the percentage loss of signal at 1 hour was calculated. For quantification of lymphatic transport, 3 assessments were made from the data of signal enhancement versus time. These were the NIR fluorescent signal enhancement value in counts at $t = 60$ minutes, the linear slope of signal enhancement from $t = 30$ to 45 minutes in counts/min, and the transit time in minutes of the arrival of tracer to the blood circulation (set at a threshold of 100 counts of signal enhancement).

Statistics. All data are presented as mean ± SD. Means of 2 groups were compared using a 2-tailed Student's *t* test. Means of 3 groups were compared using 1-way ANOVA with Tukey's multiple comparison post hoc test. All analyses were performed using Prism v5.0 (GraphPad Software) and *P* less than 0.05 was accepted as statistically significant.

Study approval. All experiments were carried out in accordance with animal protocols approved by Kantonales Veterinaramt Zurich (protocol: 237/2013).

Author contributions

STP, DA, JCL, and MD conceived and designed the study. STP, DA, and QM performed the experiments and analyzed the data. STP, DA, QM, JCL, and MD drafted the manuscript. All authors have approved the final version of the manuscript and have agreed to be accountable for all aspects of the work.

Acknowledgments

Address correspondence to: Steven T. Proulx, Institute of Pharmaceutical Sciences, Swiss Federal Institute of Technology, ETH Zurich, Vladimir-Prelog-Weg 1-5/10, HCI H398, CH-8093 Zürich, Switzerland. Phone: 41.44.633.9412; E-mail: steven.proulx@pharma.ethz.ch.

1. Alitalo K. The lymphatic vasculature in disease. *Nat Med*. 2011;17(11):1371–1380.
2. Munn LL, Padera TP. Imaging the lymphatic system. *Microvasc Res*. 2014;96:55–63.
3. Proulx ST, et al. Quantitative imaging of lymphatic function with liposomal indocyanine green. *Cancer Res*. 2010;70(18):7053–7062.
4. Karlsen TV, McCormack E, Mujic M, Tenstad O, Wiig H. Minimally invasive quantification of lymph flow in mice and rats by imaging depot clearance of near-infrared albumin. *Am J Physiol Heart Circ Physiol*. 2012;302(2):H391–H401.
5. Karaman S, Buschle D, Luciani P, Leroux JC, Detmar M, Proulx ST. Decline of lymphatic vessel density and function in murine skin during aging. *Angiogenesis*. 2015;18(4):489–498.
6. Chong C, et al. In vivo visualization and quantification of collecting lymphatic vessel contractility using near-infrared imaging. *Sci Rep*. 2016;6:22930.
7. Ogata F, Azuma R, Kikuchi M, Koshima I, Morimoto Y. Novel lymphography using indocyanine green dye for near-infrared fluorescence labeling. *Ann Plast Surg*. 2007;58(6):652–655.
8. Unno N, et al. A novel method of measuring human lymphatic pumping using indocyanine green fluorescence lymphography. *J Vasc Surg*. 2010;52(4):946–952.
9. Sevick-Muraca EM. Translation of near-infrared fluorescence imaging technologies: emerging clinical applications. *Annu Rev Med*. 2012;63:217–231.
10. Courtice FC, Simmonds WJ. Absorption of fluids from the pleural cavities of rabbits and cats. *J Physiol (Lond)*. 1949;109(1–2):117–130.
11. Tobbia D, Semple J, Baker A, Dumont D, Semple A, Johnston M. Lymphedema development and lymphatic function following lymph node excision in sheep. *J Vasc Res*. 2009;46(5):426–434.
12. Baker A, Semple JL, Moore S, Johnston M. Lymphatic function is impaired following irradiation of a single lymph node. *Lymphat Res Biol*. 2014;12(2):76–88.
13. Pain SJ, et al. Quantification of lymphatic function for investigation of lymphedema: depot clearance and rate of appearance of soluble macromolecules in blood. *J Nucl Med*. 2002;43(3):318–324.
14. Proulx ST, et al. Non-invasive dynamic near-infrared imaging and quantification of vascular leakage in vivo. *Angiogenesis*. 2013;16(3):525–540.
15. Huggenberger R, et al. An important role of lymphatic vessel activation in limiting acute inflammation. *Blood*.

2011;117(17):4667–4678.

16. Tammela T, et al. Therapeutic differentiation and maturation of lymphatic vessels after lymph node dissection and transplantation. *Nat Med*. 2007;13(12):1458–1466.

17. Zheng W, et al. Angiopoietin 2 regulates the transformation and integrity of lymphatic endothelial cell junctions. *Genes Dev*. 2014;28(14):1592–1603.

18. Proulx ST, et al. Use of a PEG-conjugated bright near-infrared dye for functional imaging of rerouting of tumor lymphatic drainage after sentinel lymph node metastasis. *Biomaterials*. 2013;34(21):5128–5137.

19. Yoffey JM, Courtice FC. *Lymphatics, Lymph and the Lymphomyeloid Complex*. London, England: Academic Press; 1970.

20. Hall JG, Morris B, Woolley G. Intrinsic rhythmic propulsion of lymph in the unanaesthetized sheep. *J Physiol (Lond)*. 1965;180(2):336–349.

21. Markhus CE, et al. Increased interstitial protein because of impaired lymph drainage does not induce fibrosis and inflammation in lymphedema. *Arterioscler Thromb Vasc Biol*. 2013;33(2):266–274.

22. Mäkinen T, et al. Inhibition of lymphangiogenesis with resulting lymphedema in transgenic mice expressing soluble VEGF receptor-3. *Nat Med*. 2001;7(2):199–205.

23. Jeltsch M, et al. Hyperplasia of lymphatic vessels in VEGF-C transgenic mice. *Science*. 1997;276(5317):1423–1425.

24. Abu-Hijleh MF, Habbal OA, Moqattash ST. The role of the diaphragm in lymphatic absorption from the peritoneal cavity. *J Anat*. 1995;186(Pt 3):453–467.

25. Parungo CP, et al. Lymphatic drainage of the peritoneal space: a pattern dependent on bowel lymphatics. *Ann Surg Oncol*. 2007;14(2):286–298.

26. Ochsenbein AM, et al. Regulation of lymphangiogenesis in the diaphragm by macrophages and VEGFR-3 signaling. *Angiogenesis*. 2016;19(4):513–524.

27. Drinker CK. *Lane Medical Lectures: The Lymphatic System, its Past to Regulating Compositionand Volume of Tissue Fluid*. Stanford, CA: Stanford University Press; 1942: 101.

28. McGeown JG, McHale NG, Thornbury KD. The role of external compression and movement in lymph propulsion in the sheep hind limb. *J Physiol (Lond)*. 1987;387:83–93.

29. Olszewski WL, Engeset A. Intrinsic contractility of prenodal lymph vessels and lymph flow in human leg. *Am J Physiol*. 1980;239(6):H775–H783.

30. Courtice FC, Steinbeck AW. The lymphatic drainage of plasma from the peritoneal cavity of the cat. *Aust J Exp Biol Med Sci*. 1950;28(2):161–169.

31. Rusznyák I, Földi M, Szabó G. *Lymphatics and Lymph Circulation: Physiology and Pathology*. Oxford, England: Pergamon Press; 1967; 971.

32. Saunders NR, Dziegielewska KM, Møllgård K, Habgood MD. Markers for blood-brain barrier integrity: how appropriate is Evans blue in the twenty-first century and what are the alternatives? *Front Neurosci*. 2015;9:385.

33. McHale NG, Roddie IC. The effect of intravenous adrenaline and noradrenaline infusion of peripheral lymph flow in the sheep. *J Physiol (Lond)*. 1983;341:517–526.

34. Le CP, et al. Chronic stress in mice remodels lymph vasculature to promote tumour cell dissemination. *Nat Commun*. 2016;7:10634.

35. White JC, Field ME, Drinker CK. On the protein content and normal flow of lymph from the foot of the dog. *Am J Physiol*. 1933;103:34–44.

36. Ikomi F, Schmid-Schönbein GW. Lymph pump mechanics in the rabbit hind leg. *Am J Physiol*. 1996;271(1 Pt 2):H173–H183.

37. Gogineni A, et al. Inhibition of VEGF-C modulates distal lymphatic remodeling and secondary metastasis. *PLoS ONE*. 2013;8(7):e68755.

38. Moriondo A, Mukenge S, Negrini D. Transmural pressure in rat initial subpleural lymphatics during spontaneous or mechanical ventilation. *Am J Physiol Heart Circ Physiol*. 2005;289(1):H263–H269.

39. Drinker CK. *Pulmonary Edema and Inflammation; an Analysis of Processes Involved in the Formation and Removal of Pulmonary Transudates and Exudates*. Cambridge, MA: Harvard University Press; 1945.

40. Florey H. Reactions of, and absorption by, lymphatics, with special reference to those of the diaphragm. *Brit J Exp Pathol*. 1927;8(6):479–490.

41. Morris B. The effect of diaphragmatic movement on the absorption of protein and of red cells from the peritoneal cavity. *Aust J Exp Biol Med Sci*. 1953;31(3):239–246.

42. Tran L, et al. Lymphatic drainage of hypertonic solution from peritoneal cavity of anesthetized and conscious sheep. *J Appl Physiol*. 1993;74(2):859–867.

43. Iijima T, Iwao Y, Sankawa H. Circulating blood volume measured by pulse dye-densitometry: comparison with (131)I-HSA analysis. *Anesthesiology*. 1998;89(6):1329–1335.

44. Choi I, et al. Visualization of lymphatic vessels by Prox1-promoter directed GFP reporter in a bacterial artificial chromosome-based transgenic mouse. *Blood*. 2011;117(1):362–365.